

# LOAN DOCUMENT

PHOTOGRAPH THIS SHEET

DTIC ACCESSION NUMBER

LEVEL

INVENTORY

S-Band Telemetry Link Lifetime  
following a Hypervelocity Impact

DOCUMENT IDENTIFICATION

**DISTRIBUTION STATEMENT A**  
Approved for Public Release  
Distribution Unlimited

**DISTRIBUTION STATEMENT**

ACCESSION FOR

NTIS ☐ GRAM ☐  
DTIC ☐ TRAC ☐  
UNANNOUNCED ☐  
JUSTIFICATION ☐

BY

DISTRIBUTION/

AVAILABILITY CODES

DISTRIBUTION

AVAILABILITY AND/OR SPECIAL

**DISTRIBUTION STAMP**

20000814 183

DATE RECEIVED IN DTIC

DATE ACCESSIONED

DATE RETURNED

REGISTERED OR CERTIFIED NUMBER

PHOTOGRAPH THIS SHEET AND RETURN TO DTIC-FDAC

H  
A  
N  
D  
L  
E  
  
W  
I  
T  
H  
  
C  
A  
R  
E

# UNCLASSIFIED

## S-BAND TELEMETRY LINK LIFETIME FOLLOWING A HYPERVELOCITY IMPACT

D. Sandison, R. Franco, L. Marshall, J. Moore

Sandia National Laboratories

Albuquerque, NM

### Abstract

To better understand the effects of hypervelocity impact generated debris on S-band radio frequency (RF) transmission, a conical aeroshell was impacted by a Lexan projectile traveling at 6.7 km/s. RF signals from four transmitting patch antennas mounted on the target were used to measure the debris effects. The aft impact produced a back-scattered debris cloud that slowed as it moved through the 2 torr atmosphere in the evacuated blast chamber, and the debris attenuated S-band signals by 2 to 4 orders of magnitude from their preimpact values. The average velocity of the RF-inhibiting debris ranged from 0.7 to 1.1 km/s depending on the distance traveled. At an intercept altitude of 230 km, the atmospheric pressure is  $10^{-7}$  torr, there is no resistive force, and the debris should continue at its initial velocity. To gain better understanding of the chamber atmosphere effects, a simple momentum transfer model for debris slowing in a nonviscous media was used to model debris propagation. The resistive force is proportional to  $V^2$ , and an initial (exoatmospheric) velocity of 1.5 km/s was calculated. Therefore, debris velocities measured at 2 torr will overestimate telemetry link lifetimes by  $V_{\text{exo}}/V_{\text{ave}}$ , which ranges from 1.4 to 2.1 in this experiment.

### Introduction

Recording exoatmospheric, end-event data from a target that is impacted at hypervelocity requires a telemetry link that nominally lasts for  $\sim 100 \mu\text{s}$ . To better understand S-band RF transmission during impact, an antenna transmission test was conducted Aug. 25, 1999, at the Arnold Engineering Development Center (AEDC) G-Range Gas Gun Facility in Tennessee. These measurements were "piggybacked" on a planned experiment scheduled for an aft shot line.

The intent of this measurement was to directly verify the attenuation properties of the debris cloud at transmission frequencies in the 2.2 to 2.3 GHz range, which are of interest for flight test telemetry. Figure 1 depicts an impact generated debris cloud moving along the target body. When the debris reaches the S-band transmitting antennas, the received signal strength is affected. The attenuation effects of the debris cloud and its associated time of arrival can be determined by time recordings of the RF carrier power. Multiple antennas transmitting at unique frequencies were mounted on the target body to provide the spatially and temporally resolved measurements that allow for a better understanding of debris cloud dynamics.

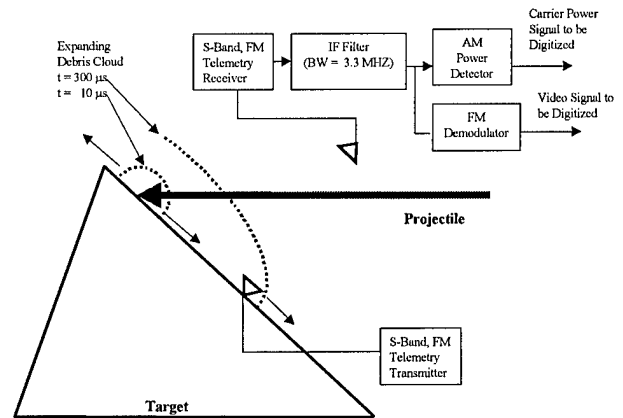


**Figure 1: RF Signal Loss Experiment. Debris generated at impact propagates along the target body and attenuates the S-band signal. Time recordings of the received carrier power capture the debris cloud time-of-arrival and attenuation effects.**

### Experiment Setup & Antenna Installation

The AEDC blast chamber is 10 ft in diameter and was evacuated to 2 torr for this experiment. The two-stage gas gun fired a Lexan projectile at 6.7 km/s into a target that was suspended from the ceiling with mounting string as shown in Figure 2.

Accounting for the 40° impact angle and the projectile size, the target was first struck approximately 14 cm from the target base (measured along the aeroshell). The point of first contact was about 6 cm forward of the shot line marked by the cross in Figure 3 (left).

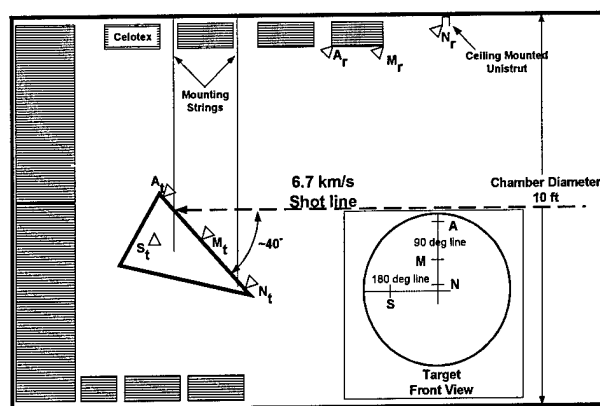


**Figure 2: Chamber Setup** Location of target within blast chamber.  $A_t$ ,  $M_t$ ,  $N_t$ , and  $S_t$  are the aft, midbody, nose, and side transmitters respectively.  $A_r$ ,  $M_r$ ,  $N_r$  are receiving antennas.  $S_r$  is mounted to the chamber wall directly opposing its transmitter and is not shown.

Four S-Band transmitting patch antennas were mounted at intervals along the target as shown in Figure 2. Each link was modulated with a 625 KHz sine wave; Table 1 summarizes the operating frequencies and antenna placement for each of the RF links. The target antennas were taped to the target surface as shown for the aft antenna in

Figure 3 (left). The printed circuit board used for the transmitting antennas was DiClad 522 as dimensioned in Figure 3 (right). The shaded area in Figure 3 is 0.062 inch thick copper.

Each receiving antenna was mounted so that it directly faced its corresponding target-mounted transmitting antenna. The antenna mounting is designed to offer direct line of sight to the corresponding transmission antennas on the test unit. This alignment insures a well-defined coupling path between the antenna pairs, so that the debris disturbance effects dominate the variation in signal power during the event. All antennas were linearly polarized. Antennas  $A_r$  and  $M_r$  are mounted to the Celotex material hanging underneath the chamber ceiling, and  $N_r$  is twist-tied to a piece of ceiling mounted unistrut. The side-mounted receiver ( $S_r$ ) is attached to the chamber wall directly opposite its transmitter ( $S_t$ ).

## **RF Instrumentation & Measurements**

### **RF Measurement and Recording Requirements**

The performance diagnosis of the RF telemetry links with debris cloud disturbance is based on a Received Signal Strength Indicator (RSSI) measurements made for each of the four data links. Each channel was sampled at 0.2  $\mu$ s intervals with 8 bit resolution. The recorded time window runs from 10 ms before to 90 ms after impact.

**Table 1: RF Frequencies & Antenna Placement\***

RF Transmission Experiments on Debris Cloud Experiment			
Link	Frequency (MHz)	Distance from Target Base Measured along the Aeroshell (cm)	RX Antenna Distance (cm)
A (Aft)	2268.5	2.5	135
M (Midbody)	2250.5	46	160
N (Nose)	2288.5	82	211
S (Side)	2209.5	13	~90

\* all transmission bandwidths were 2 MHz.

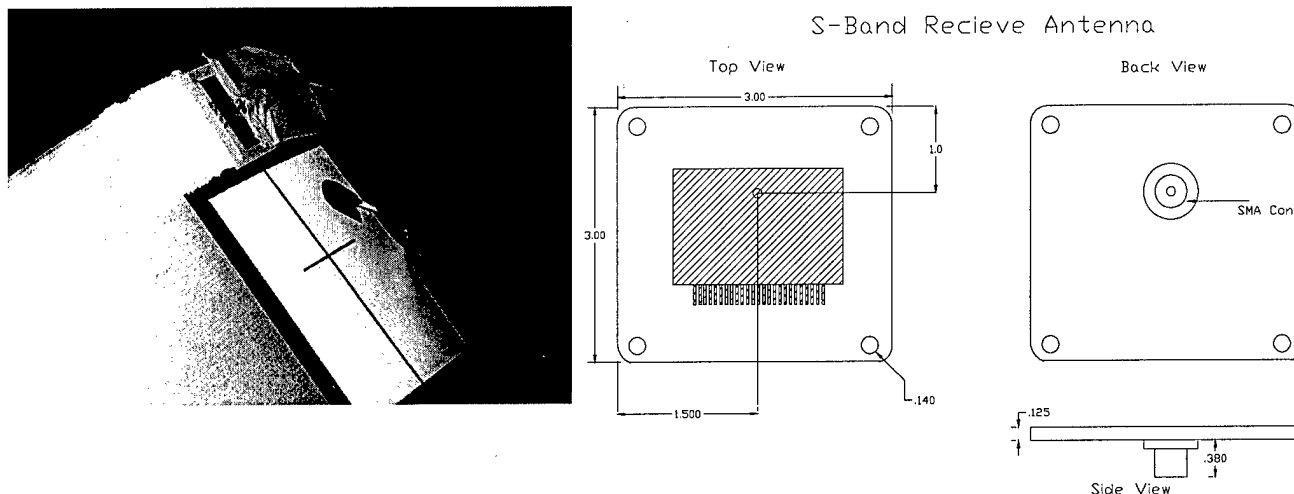


**Figure 3: Transmitting Antennas As Attached In The Experiment (left) aft antenna mounted to target, (right) antenna schematic.**

The time of arrival (TOA) analysis of this data offers insight into the propagation speed of the debris cloud following impact. This TOA analysis relies heavily on time synchronization of the signals recorded from each link, so all of the digitizers used a common trigger input.

### RF Instrumentation & Recording Setup

The instrumentation and recording setup for this experiment was driven by the separation of the test unit and the receiver and transmitting antenna pairs inside the vacuum chamber from the receiving and digitizing equipment outside the chamber (see Figure 4). Note that the RF transmitters (i.e. RF signal sources) were located outside the chamber and were cabled to the transmitting antennas on the test unit through 20' of RG58 outside the chamber and 25' of RG142 inside the chamber.

The transmitters driving these antennas all had nominal power output of 2.0 watts. The power loss through the transmitter cable at S-Band is about 15 dB. Thus, the power supplied to the transmitting antennas is about +19 dBm. The RF power at the receiver inputs was too high for unsaturated operation, and a 10-dB, SMA pad was inserted at the receiver inputs. This correction brought the receivers into proper operating input power.

The transmitters were battery powered to avoid the potential for ground loops or noise coupled through gun actuation signals. The transmitter case and the receiver rack were physically separated by about 30 feet to limit extraneous signal coupling.

The IF filters were set to 3.3 MHz, which demonstrated good stability in the signal reception. Detailed calibration methods and values are reported elsewhere<sup>1</sup>.

To demonstrate that signal fluctuations in one channel did not couple into another, cross talk tests were performed with all transmitter/receiver combinations (12 possible). With antennas, transmitters, and receivers in their experimental configuration and inside the chamber, two of the RSSI signals were monitored simultaneously on a storage oscilloscope. No cross talk was detected in this checkout.

## Results

### Data Recordings

On-site LeCROY digitizers captured voltage data for each of the recorded channels, and AEDC provided ASCII files for each channel. The digitizer that recorded the RF signal strength for the side antenna had a stuck bit, which produced flat spots in its trace.

### RF Signal Loss

Figure 5 shows the RF power versus time for each antenna. The aft antenna was destroyed at impact; its signal drops by ~40 dB (four orders of magnitude) and never recovers. Signal levels on the side, nose, and mid antennas drop by 25 – 35 dB for ~7 ms. After 7 ms, the average RF power returns to near its preimpact level for the nose and mid antennas but with large amplitude fluctuations.

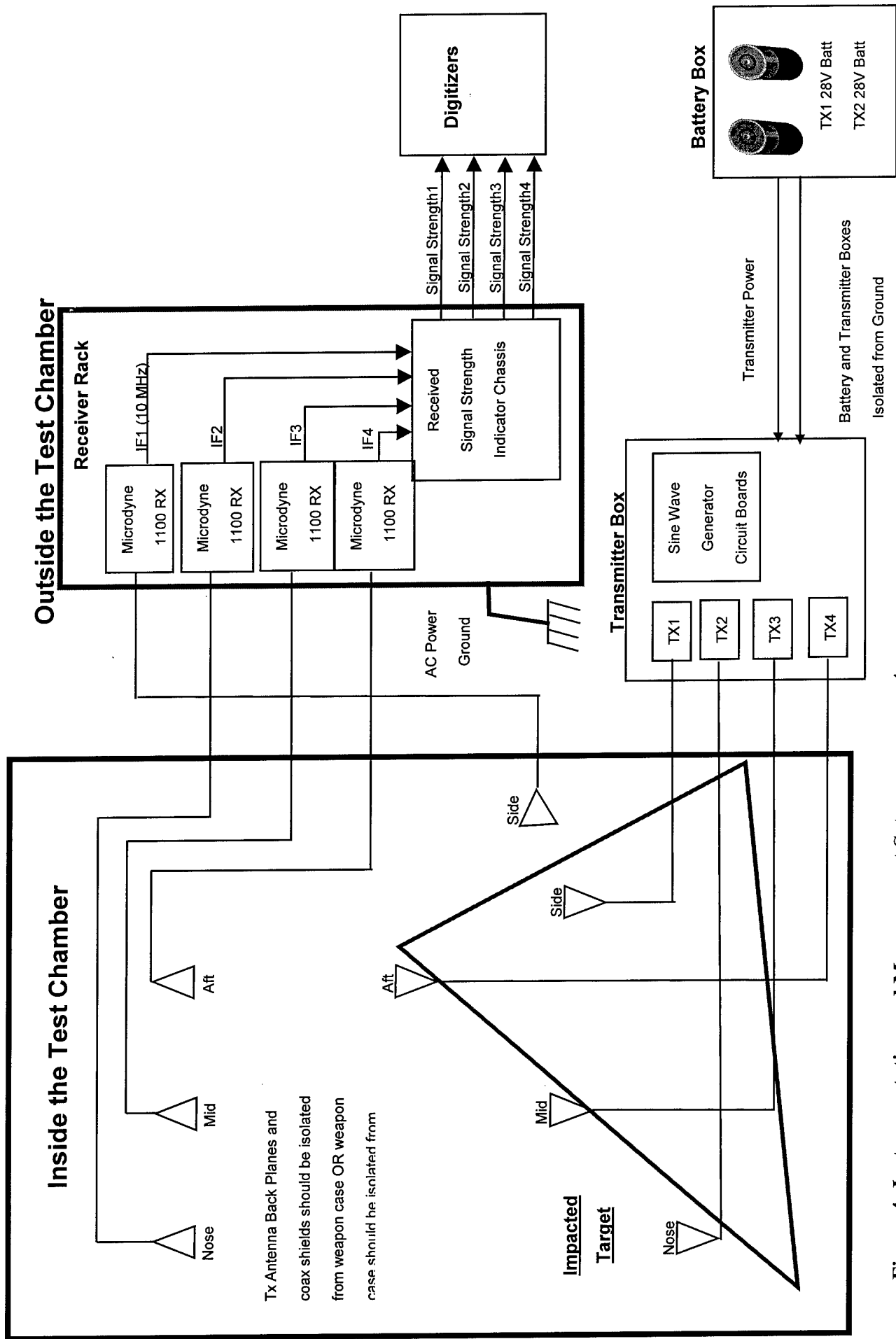


Figure 4: Instrumentation and Measurement Setup

# UNCLASSIFIED

**Figure 6** shows the S-band signal demise from aft antenna loss to 1500  $\mu$ s. The signal dips at *a* and *b* mark the projectile passing between the nose and midbody transmitter/receiver pairs. The temporal separation of these events ( 70  $\mu$ s) and the spatial separation of their RF paths (0.47 m) match the 6.7 km/s projectile velocity.

The projectile hit the target near the aft antenna, destroying it at about 10  $\mu$ s after impact. The midbody transmitter suffered only ~10dB fluctuations until its signal was lost at ~300  $\mu$ s after impact. The forward transmission remained strong until 700  $\mu$ s after impact, and its signal was lost at 1000  $\mu$ s after impact. The signal loss curves for the midbody and nose antennas also show that the debris cloud is slowing as it propagates in the chamber. The average debris velocity from the impact point to the midbody occlusion is (32 cm)/(300  $\mu$ s) = 1.1 km/s,

and the average debris velocity from the impact point to the nose is (69 cm)/(1000  $\mu$ s) = 0.69 km/s.

## Analysis

This experiment indicates the passing of an impact generated debris cloud that is decelerating in the 2 torr chamber atmosphere. To gain a better understanding of the chamber atmosphere effects, a simple momentum transfer model is used for debris slowing in a nonviscous media

$$m \frac{dV}{dt} = -\frac{1}{2} \rho_c A V^2, \quad \text{Equation 1}$$

where *m* is the debris particle mass, *V* its velocity, *A* its effective cross sectional area, and  $\rho_c$  is the chamber air density<sup>2,3</sup>.

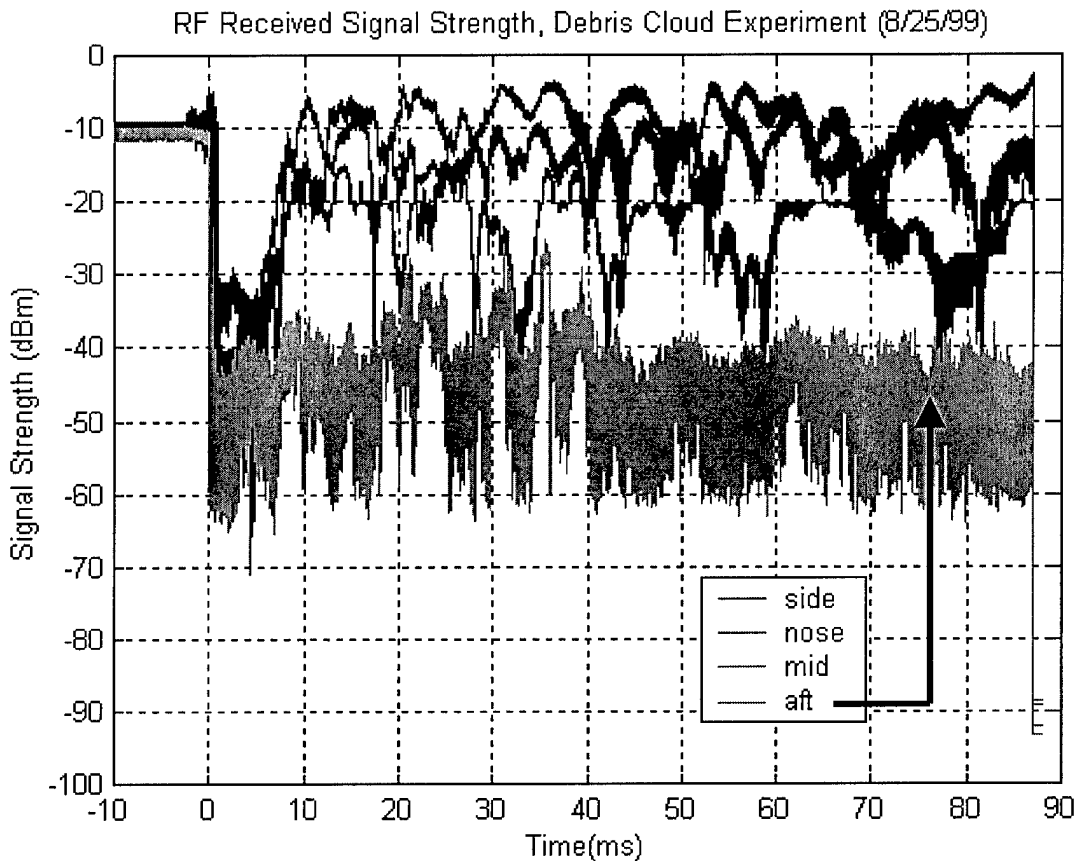


**Figure 5:** Received RF Signal Strength versus time. Aft antenna signal loss is shown as *t* = 0, and dBm is dB referenced to 1 mW.

# UNCLASSIFIED

Defining the constant  $a = \frac{\rho_c A}{2m}$  and initial velocity

as  $V_0$ , and setting  $X(0) = 0$ , equation 1 can be integrated once to find particle velocity ( $V$ ) and twice to find particle position ( $X$ ) as a function of time. By measuring the debris time-of-arrival ( $X(t)$ ) at two points, the following simultaneous equations can be solved for  $a$  and  $V_0$ :

$$X(t_1) = \frac{1}{a} \ln(1 + aV_0 \cdot t_1) \quad \text{Equation 2}$$

$$X(t_2) = \frac{1}{a} \ln(1 + aV_0 \cdot t_2). \quad \text{Equation 3}$$

The backscattered debris velocity results are summarized in Table 2. The average debris velocity ( $V_{ave}$ ) is calculated by dividing distance from impact

( $X$ ) by signal-loss time ( $t$ ). Since atmospheric resistance slows the debris,  $V_{ave}$  decreases with distance from the impact.

Simultaneously solving equations 3 and 4 using the midbody ( $X(300 \mu s) = 0.32 \text{ m}$ ) and nose ( $X(1000 \mu s) = 0.69 \text{ m}$ ) yields atmospheric correction constants values of  $a = 2.0 \text{ m}^{-1}$  and  $V_0 = 1.5 \text{ km/s}$ . At an exoatmospheric intercept at an altitude of 230 km,  $a$  is scaled by  $\rho_{exo}/\rho_{chamber} = 5 \times 10^{-8}$ , and exoatmospheric debris propagates at its initial velocity (1.5 km/s in this case) without appreciable slowing.

Using this model, the chamber RF signal loss time is corrected for chamber atmosphere effects by multiplying the chamber time by  $V_{ave}/V_0$ . For an aft hit, the chamber results overestimate the lifetime of the midbody signal by 30% and the nose signal by 50%.

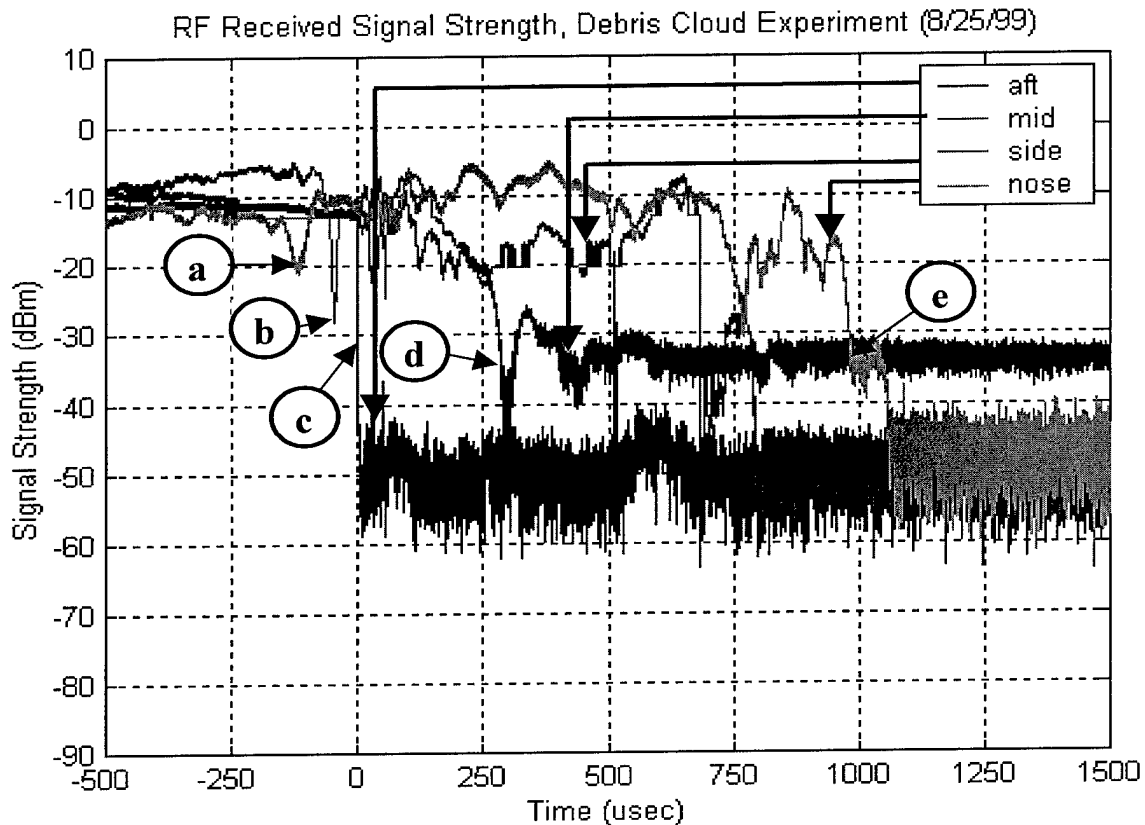


**Figure 6: Received Rf Signal.** Records start from 500  $\mu s$  before to 1500  $\mu s$  after aft antenna loss. a) -115 $\mu s$ , b) -45  $\mu s$ , c) = impact  $\pm 10 \mu s$ , d) ~ 290  $\mu s$ , e) ~ 990 $\mu s$  (add 10  $\mu s$  to each time to calculate time after impact).

# UNCLASSIFIED

**Table 2: Backscattered Debris Results From This Test.**

Antenna	t ( $\mu$ s) (@2 torr)	X (m)	V <sub>average</sub> (km/s)	Atmospheric Correction Constants	t ( $\mu$ s) (@10 <sup>-7</sup> torr)
Midbody	300	0.32	1.1	V <sub>0</sub> = 1.5 km/s a = 2.0 m <sup>-1</sup>	210
Nose	1000	0.69	0.7		460

## Conclusions

These results demonstrate a backscattered debris cloud that

- 1) occludes S-band transmissions as it passes,
- 2) has a duration of a few milliseconds, and
- 3) slows as it interacts with the chamber atmosphere.

The S-band RF power is steeply attenuated when the debris reaches the antenna, and the milliseconds that it took for the debris cloud to pass would block end-event data transmission from a hypervelocity impact. Therefore, avoiding the debris is the most viable strategy for end-event telemetry.

A simple, physical air resistance model can be used to explain the debris slowing and a backscattered initial velocity of 1.5 km/s was calculated. If these results hold true, then a ground antenna that observes the intercept from the impact-side is severely limited, and multiple data collection options must be seriously considered.

It is interesting that the debris cloud interfered with a magnetic gauge next to the nose antenna within microseconds of RF signal loss, and the magnetic interference stopped when the RF signal returned. Similar gauges on the bottom of the target were not affected. A debris cloud composed of moving charged particles would provide a simple explanation for the correlated effects. However, this is not a simple problem, and the exact nature of the debris is still unknown.

The S-band signal loss results highlight two well-known but persistent problems associated with evacuated chamber tests:

- 1) the chamber atmosphere is orders-of-magnitude more dense than at intercept altitude,
- 2) the subscale target impacted by a hydrocarbon polymer (Lexan) projectile does not accurately represent the complex interaction of real exoatmospheric intercepts.

Collecting additional debris cloud data at AEDC could validate a model that allows chamber results to be extrapolated to exoatmospheric intercepts. This predictive power would allow key telemetry design decisions to be made for post-impact data collection.

## Acknowledgements

The authors wish to thank the U.S. Army LFT&E Program for allowing us to participate in the test that was sponsored by the U.S. Army NMD Gas Gun Program.

We also thank Jeff Scheffer (15425), Matthew Sena and Chris Gallegos (02343), and John Stanalonis (15415) for data collection, antenna development, and chamber setup, Gary Ashcraft (02662) and Clint Landrón (02664) for analysis support, and Dianna Trujillo (02661) for manuscript preparation.

Sandia is a multiprogram laboratory operated by Sandia Corporation, a Lockheed Martin Company, for the United States Department of Energy under Contract DE-AC04-94AL8500.

## References

- 1) R J. Franco, J. W. Moore, D. R. Sandison "Hypervelocity Impact Debris-Cloud Effects On Radio Frequency (Rf) Signal Transmission", SAND2000-1215, May 2000
- 2) Marvin E. Backman and Verneer Goldsmith, "The Mechanics of Penetration of Projectiles into Targets", Int. J. Engng Sci. 1978. Vol. 16, pp 1-99. (eqn. 3.6)
- 3) M.E. Kipp, D.E. Grady, J.W. Swegle, "Experimental and Numerical Studies of High-Velocity Impact Fragments", SAND93-0773, August 1993 (eqn 5).